CHEMICAL ENGINEERING TRANSACTIONS
VOL. 70, 2018
A publication of AIDIC
The Italian Association of Chemical Engineering
Online at www.aidic.it/cet
Guest Editors: Timothy G. Walmsley, Petar S. Varbanov, Rongxin Su, Jiří J. Klemeš

ISBN 978-88-95608-67-9; **ISSN** 2283-9216
DOI: 10.3303/CET1870066

Modelling and Simulation of Zinc-air Flow Battery with Zinc Regeneration Process

Woranunt Lao-atiman[a], Soorathep Kheawhom[a,b*]

[a]Department of Chemical Engineering, Faculty of Engineering, Chulalongkorn University, Bangkok 10330, Thailand
[b]Research Unit of Computational Process Engineering, Chulalongkorn University, Bangkok 10330, Thailand
soorathep.k@chula.ac.th

Reliable and low-cost electrical energy storage systems are required for grid integration of various intermittent sources of renewable energy. Zinc-air flow batteries have shown high potential for electricity storage application because of their high energy density at low cost. The flow batteries can reduce significantly the problem associated with the formation of dendritic zinc during recharge and the formation of a passivation film during discharge. The aims of this work include the development of mathematical models of a zinc-air flow battery (ZAFB). The developed model was implemented in MATLAB and validated with experimental data. The models were then used to investigate the behavior of the flow battery. The concentration of potassium hydroxide in the electrolyte, as well as the feed flow rate considerably affected the performance of ZAFB.

1. Introduction

Renewable energy technologies have been continuously being developed because of pressure on environmental awareness and accessibility limitations of fossil fuel. However, renewable energy has intermittent characteristic. Thus, the grid integration of various intermittent sources of renewable energy requires reliable and low cost electrical energy storage systems.

Zinc-air batteries have shown high potential as an electrical energy storage system because of their high energy density at low cost (Xu et al., 2015). Besides, zinc is an attractive anode material because it is lightweight, non-toxic, inherently safe, inexpensive and readily available. In addition, the use of atmospheric oxygen as their cathode material is advantageous (Suren and Kheawhom, 2016). The batteries generate electricity through the electrochemical reaction of zinc and oxygen. The battery can be recharged electrically using electricity from an external source. An important problem related to the zinc electrode in rechargeable cells is the formation of dendrites during the recharging of the cell which is an important life cycle-limiting factor for rechargeable zinc-based batteries (Pei et al., 2014). One approach to overcome this problem, is the use of a battery with flowing electrolyte configuration which reduces significantly the problem associated with the formation of dendrites. The zinc-air flow batteries are configured to act as an energy storage and conversion system. Zinc granules serving as the reactant are stored in a storage tank and fed to the cell. Also, the electrolyte stored in other storage tanks can be fed to the cell separately. During discharge, zinc granules react with hydroxide ion in the electrolyte, and produce zinc oxide. The discharge product is then removed from the cell. The discharge stream containing zinc oxide is fed to the regeneration process to convert back to zinc granules.

Experimental investigation of significant parameters influencing the performance of the batteries are time-consuming. Therefore, mathematical modeling and simulation can be very helpful in defining critical design parameters for the system. Besides, the models are required for optimization and smooth operation. Xiao et al. (2016a) experimentally examined a continuous zinc-air battery. Also, the embedded control system based on microcontroller for this system was developed (Xiao et al., 2016b). Previously, mathematical models of a primary zinc-air battery (Mao, 1992) and a rechargeable zinc-air battery (Deiss et al., 2002) were developed. Besides, the effects of parameters air-composition were numerically studied (Schröder and Krewer, 2014). Nevertheless, a mathematical model of zinc-air flow batteries (ZAFBs) has not been developed.

Please cite this article as: Lao-atiman W., Kheawhom S., 2018, Modelling and simulation of zinc-air flow battery with zinc regeneration process , Chemical Engineering Transactions, 70, 391-396 DOI:10.3303/CET1870066

The aims of this work include the development of mathematical model of a zinc-air flow battery integrating with zinc regeneration process. The developed model was implemented in MATLAB and validated with experimental data. It was then used to investigate the behaviour and to evaluate the performance of the system. Most importantly, the model was used to improve our insight on the zinc-air flow battery and zinc regeneration process. Moreover, the effects of various different operating conditions including temperatures, different concentration and composition of the zinc anode, different current densities and different flow rates were then investigated. The integration system between zinc-air flow battery and zinc regeneration process showed high potential candidate as a cost-effective energy storage system.

2. Zinc-air flow battery

ZAFB is a galvanic cell consisting of two electrodes (anode and cathode). The schematic diagram of ZAFB is shown in Figure 1a. The anode active material is zinc (Zn). Potassium hydroxide (KOH) is commonly used as an electrolyte. Overall reaction at the anode consumes zinc and hydroxide ion (OH^-), supplied from the electrolyte, and simultaneously produces zinc oxide (ZnO) and water (H_2O). At the cathode, the active material is oxygen (O_2) from ambient air. Oxygen reduction reaction (ORR), simultaneously consuming O_2 and H_2O and producing OH^-, is occurred. Thus, H_2O, produced at the anode, transfers across the cell and refills H_2O consumed at the cathode. On the contrary, OH^-, produced at the cathode, transports through the separator membrane and replenishes OH^- consumed at the anode (Wongrujipairoj et al., 2017).

$$Zn+2OH^- \rightarrow ZnO+H_2O+2e^-$$

$$O_2+2H_2O+4e^- \rightarrow 4OH^-$$

Figure 1b depicts a schematic diagram of ZAFB integrating with an electrolyser. Zinc particles suspended in an electrolyte is fed into ZAFB. The discharge from ZAFB contains $Zn(OH)_4^{2-}$, ZnO and the electrolyte. Regeneration of the zinc particles is carried in the electrolyser.

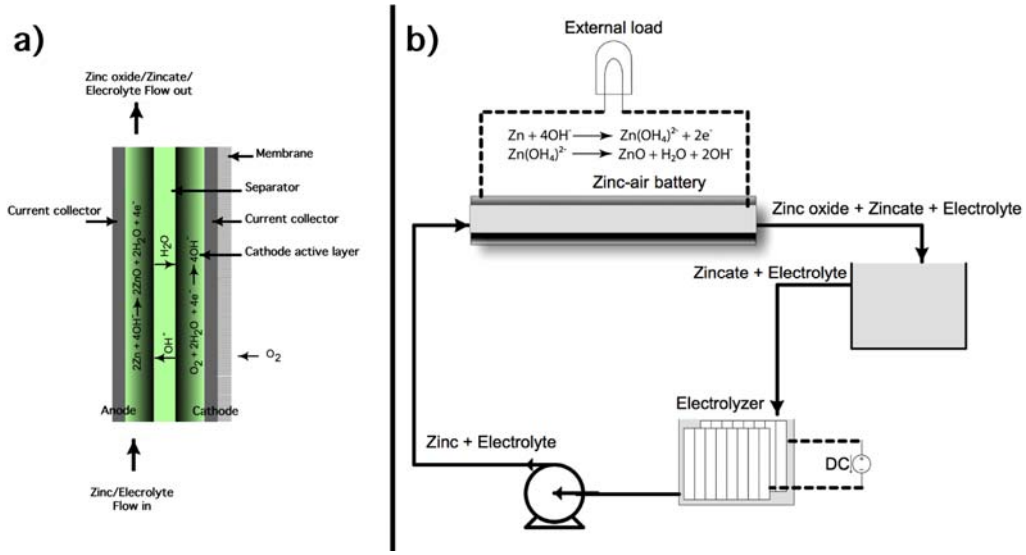

Figure 1: A schematic diagram of a) ZAFB, and b) ZAFB integrated with an electrolyzer.

3. Mathematical models of ZAFB

The models were developed and implemented using MATLAB. The assumptions have been made including; (1) isothermally operation at 298.15 K, (2) zero-dimension model, (3) no concentration gradient, (4) negligible distance between the cells, (5) constant physical properties, electrode areas and thickness, (6) zinc dissolution taking place only at the anode and oxygen reduction reaction (ORR) taking place only at the cathode, (7) Quasi-electroneutrality, (8) ideal gas behavior, and (9) binary mass diffusion.

The molar balance of species k at electrode j is expressed as in Eq(1). N_k is mole of species k, C_k is concentration of species k and $V_{electrolyte}$ is an electrolyte volume. A molar transfer rate across the electrodes of species k (J_k) is expressed as the summation of diffusion (J_k^{diff}), migration (J_k^{mig}) and convection (J_k^{conv})) molar

flow rates. $z_k^{\pm}$ is ion number of the species. F_{conv} is the convective volume flow. Thus, Eq(1) can be rearranged as in Eq(6), where F_k is a molar flow rate of species k and r_i is rate of reaction i.

$$dN_k^j / dt = C_k^j (dV_{\text{electrolyte}}^j / \text{dt}) + V_{\text{electrolyte}}^j (dC_k^j / \text{dt}) \tag{1}$$

$$J_k = J_k^{\text{diff}} + J_k^{\text{mig}} + J_k^{\text{conv}} \tag{2}$$

$$J_k^{\text{diff}} = D_k ((c_k^{\text{cathode}} - c_k^{\text{anode}}) / \delta_{\text{sep}}) \varepsilon^{\text{sep}} A^{\text{sep}} \tag{3}$$

$$J_k^{\text{mig}} = (t_k / z_k^{\pm} F) i^{\text{cell}} \varepsilon^{\text{sep}} A^{\text{sep}} \tag{4}$$

$$J_k^{\text{conv}} = F_{\text{conv}} c_k^{\text{anode}} \tag{5}$$

$$dC_k^j / dt = (F_{k,\text{in}} - F_{k,out} + J_k^{\text{diff}} + J_k^{\text{mig}} + J_k^{\text{conv}} + \sum_i v_{k,i} r_i - C_k^j dV_{\text{electrolyte}}^j / dt) / V_{\text{electrolyte}}^j \tag{6}$$

From quasi-electroneutrality assumption, the positive ion can be calculated by ionic species charge balance. The accumulation of Zn and ZnO is expressed by molar balance as in Eq(9) and Eq(10), where r_1 and r_2 are the rates of Zn dissolution and ZnO precipitation. The rates of Zn dissolution and ORR are direct proportion to the electrical current. In comparison, ZnO precipitation is defined by solubility.

$$\sum_k z_k^{\pm} C_k^j = 0 \tag{7}$$

$$C_{K^+}^j - C_{OH^-}^j - 2C_{Zn(OH)_4^{2-}}^j = 0 \tag{8}$$

$$dN_{ZnO} / dt = F_{ZnO,\text{in}} - F_{ZnO,\text{out}} + v_{ZnO} r_2 \tag{9}$$

$$dN_{Zn} / dt = F_{Zn,\text{in}} - F_{Zn,\text{out}} + v_{Zn} r_1 \tag{10}$$

$$r_1 = i_{Zn} (A_{\text{anode}} / n_e F) \tag{11}$$

$$r_2 = k_s \left(C_{Zn(OH)_4^{2-}} - C_{Zn(OH)_4^{2-}}^{\text{sat}} \right) \tag{12}$$

Where k_s is the rate constant of r_2 reaction and $C_{Zn(OH)_4^{2-}}^{\text{sat}}$ is the saturation concentration of zincate ion. The volume of each species is calculated from partial molar volume. The volume of the anode is the summation of the volume of zinc, zinc oxide and carbon.

$$V_{\text{solid}}^{\text{anode}} = N_{Zn} \bar{V}_{Zn} + N_{ZnO} \bar{V}_{ZnO} + N_{carbon} \bar{V}_{carbon} \tag{13}$$

$$dV_{\text{solid}}^{\text{anode}} / dt = \bar{V}_{Zn} (dN_{Zn} / \text{dt}) + \bar{V}_{ZnO} (dN_{ZnO} / \text{dt}) \tag{14}$$

$$V_{\text{electrolyte}}^{\text{anode}} = \sum_k N_k^{\text{anode}} \bar{V}_k \tag{15}$$

$$dV_{\text{electrolyte}}^{\text{anode}} / dt = \sum_k \left(V_{\text{electrolyte}}^{\text{anode}} dC_k^{\text{anode}} / dt + C_k^{anode} dV_{\text{electrolyte}}^{\text{anode}} / dt \right) \tag{16}$$

The volume transfers between two electrodes, calculated from molar transfer rate J_k, is used to express the electrolyte volume of the cathode.

$$F_{conv} = \sum_k J_k \bar{V}_k \tag{17}$$

Where F_{conv} is a convective flow, defined as the volume of electrolyte flow from the cathode to the anode. F_{conv} has a positive sign at the anode and negative sign at cathode. The change of electrolyte volume at the cathode is expressed as in Eq(18). r_3 is the rate of ORR.

$$dV_{\text{electrolyte}}^{\text{cathode}} / dt = -F_{conv} + r_3 \sum_k \nu_k \bar{V}_k \tag{18}$$

The cell potential (E_{cell}) of ZAFB is calculated from Nernst potential (E^0_{cell}) subtracted by the overpotentials and different losses as expressed in Eq(19).

$$E_{\text{cell}} = E^0_{\text{cell}} - \eta^{\text{anode}}_{\text{activation}} - \eta^{\text{cathode}}_{\text{activation}} - \eta^{\text{ade}}_{\text{activation}} - \eta_{\text{ohmic}} - \eta^{\text{sep}}_{\text{ionic}} - \eta_{conc} \tag{19}$$

$$E^0_{\text{cell}} = \left[0.041 + \frac{RT}{z_e^{\text{cathode}} F} \ln \left(\frac{\frac{P_{O_2}}{P^{\text{ref}}}}{\left(\frac{C^{\text{cathode}}_{OH^-}}{C^{\text{ref}}} \right)^4} \right) \right] - \left[-1.266 + \frac{RT}{z_e^{\text{anode}} F} \ln \left(\frac{\frac{C^{\text{anode}}_{Zn(OH)_4^{2-}}}{C^{\text{ref}}}}{\left(\frac{C^{\text{anode}}_{OH^-}}{C^{\text{ref}}} \right)^4} \right) \right] \tag{20}$$

The activation loss is expressed in the term of inverse hyperbolic sine as in Eq(21). i_0 is the rate of current proceeded at reaction equilibrium. α is charge transfer coefficient. Commonly, α is 0.5 with assumption of symmetrical electron transfer. The exchange current density is determined from experiments. However, the temperature influence is neglected because of isothermal condition.

$$\eta_{\text{activation}} = (2RT / z_e F) \sinh^{-1}((e^{(\alpha z_e F \eta / \text{RT})} - e^{(-(1-\alpha) z_e F \eta / \text{RT})}) / 2) \tag{21}$$

$$i_0^{\text{anode}} = i_0^{\text{anode,ref}} a_0 ((1-\varepsilon) / (1-\varepsilon_0))^{2/3} \delta_{\text{anode}} (V^{2/3}_{\text{solid},Zn} / (V^{2/3}_{\text{solid},Zn} + V^{2/3}_{\text{solid},ZnO})) \tag{22}$$

Where $i_0^{\text{ref, anode}}$ is the reference exchange current density, determined by fitting of experimental data. δ_{anode} is the thickness of the anode? The effective exchange current density for the cathode (i_0^{cathode}) is expressed as a function of an active surface area of catalyst per unit volume (a_c), an active thickness (δ_{active}), and an oxygen concentration.

$$i_0^{\text{cathode}} = i_0^{\text{cathode,ref}} a_c \delta_{\text{active}} (P_{O_2} / P^{\text{ref}}) \tag{23}$$

The ohmic loss is expressed by the ohmic law. The total ohmic resistance (R_{ohmic}) is calculated from conductivity (σ) and molar fraction (χ) of each species involved. Also, ion transport resistance in the separator contributes to the ohmic potential loss.

$$\eta_{\text{ohmic}} = i^{\text{cell}} A^{\text{cell}} \left[\frac{\delta_{\text{anode}}}{\sigma_{\text{anode}} A_{\text{anode}}} + \frac{\varepsilon^{1.5} \delta_{\text{electrolyte}}}{\sigma_{\text{electrolyte}} A_{\text{electrolyte}}} + \frac{\delta_{\text{cathode}}}{\sigma_{\text{cathode}} A_{\text{cathode}}} + R_{\text{comp}} \right] \tag{24}$$

$$\sigma_{\text{anode}} = \chi_{Zn} \sigma_{Zn} + \chi_{ZnO} \sigma_{ZnO} + \chi_{carbon} \sigma_{carbon} \tag{25}$$

$$\eta^{\text{sep}}_{\text{ionic}} = -((-i_{\text{cell}} - F B_1 / \delta_{\text{sep}} + F F_{\text{conv}} B_3 / \varepsilon^{\text{sep}} A^{\text{sep}}) / (F^2 B_2 / \text{RT})) \delta_{\text{sep}} \tag{26}$$

$$B_1 = \sum_k z_k^{\pm} D_k \left(C_k^{\text{cathode}} - C_k^{\text{anode}} \right) \tag{27}$$

$$B_2 = \sum_k z_k^{\pm 2} D_k \overline{C_k} \tag{28}$$

$$B_3 = \sum_k z_k^{\pm} C_k^{\text{anode}} \tag{29}$$

The concentration loss is the loss occurred from mass transfer limit of the reactant, in this case oxygen at the cathode. The concentration loss is calculated from limiting current density (i_{lim}), resulted from oxygen transfer rate limit. z_{e,O_2} is the number of exchanged electrons per one molecule of reacting oxygen.

$$\eta_{conc} = (\text{RT} / z_{e,O_2} F) \ln \left(1 - (i^{\text{cell}} / i^{\text{lim}}) \right) \tag{30}$$

4. Model validation and simulation results

Polarization characteristic of the battery is presented in Figure 2a, the voltage of the battery is linearly dependent of the discharged current density, indicating that ohmic losses dominated the cell performance. The cell voltage decreases as the current density increases. In comparison, the power of the cell increases as the current density increases and reaches the maximum at the discharge current density of 20 mA/cm^2. The simulation results are in an acceptable agreement with experimental data. Small offset was observed at high current density above normal operating region. The effects of KOH concentration are presented in Figure 2b. The solubility of zinc oxide generally increases with the increasing of KOH concentration (Gilliam et al., 2007). However, the increase in KOH concentration increases its viscosity, consequently decreases the transfer rate of hydroxide ion. At low current density, the cathode activation loss, which is dependent of KOH concentration, is dominated. As in Figure 2c, increasing in KOH concentration from 4 to 8 M decreases the anode activation loss. However, a significant increase of the anode activation loss is observed at 14 M because $i_0^{anode,ref}$ increase along with KOH concentration until the maximum point at 7 M KOH. Increasing KOH concentration further results in declining of $i_0^{anode,ref}$. At high current density, high KOH concentration exhibits low performance because of ohmic loss which is mainly affected by KOH concentration. Thus, the optimum KOH concentration was found to be 8 M. Previous study by Sapkota and Kim (2010) also reported similar results. Figure 2d shows the effects of feed flow rate at a constant discharge current of 15 mA/cm^2. Cell voltage depends on mole of Zn in ZAFB. The non-flowing cell operates like a battery with finite amount of Zn. The amount of Zn decreases with the time. The depletion of Zn results in dropping of cell voltage. Increasing the flow rate results in extension of discharge duration.

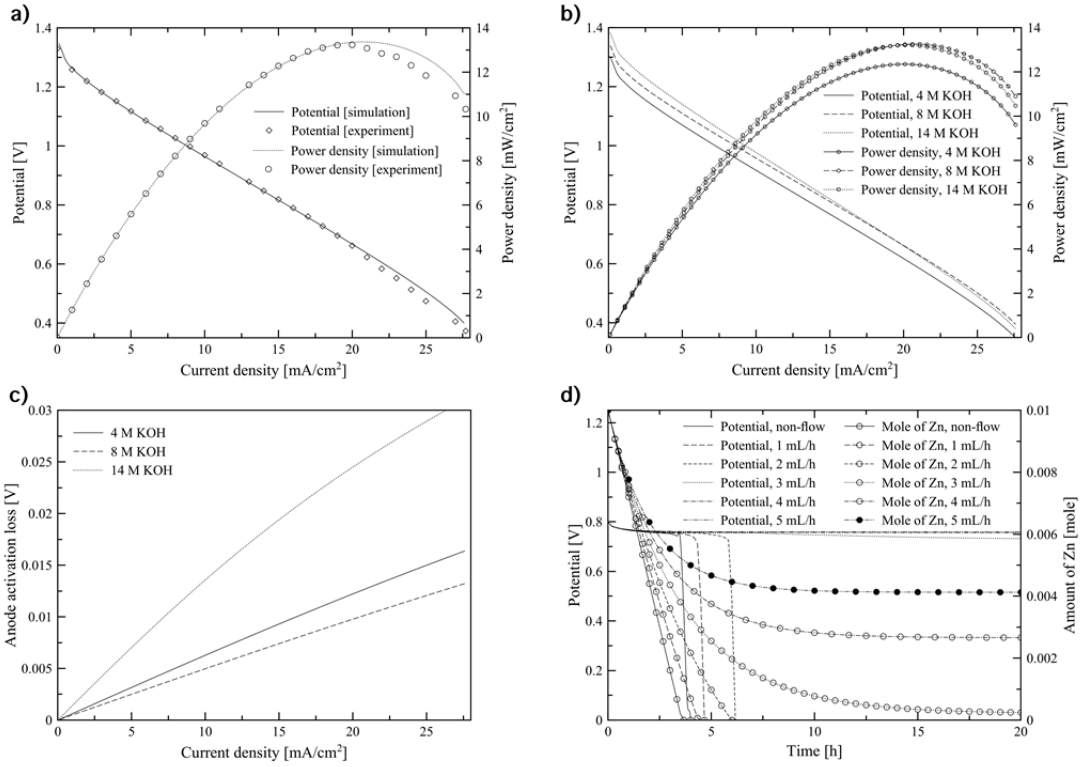

Figure 2: a) validation of the models, b) the effects of KOH concentration, c) the effects of KOH on the anode activation loss, and d) the effects of feed flow rate.

5. Conclusions

Mathematical models of ZAFB were proposed. Good agreement between simulation and experimental observation was achieved. The concentration of KOH in the electrolyte and the feed flow rate considerably affected the performance of ZAFB. The optimum KOH concentration was found to be 8 M. The models improve our insight on design and operation of ZAFB and can be extended to investigate the effects of other parameters.

Acknowledgments

This research is supported by Chulalongkorn Academic Advancement into Its 2nd Century Project, Chulalongkorn University.

References

Deiss E., Holzer F., Haas O., 2002, Modeling of an electrically rechargeable alkaline Zn–air battery, Electrochimica Acta, 47, 3995-4010.

Mao Z., 1992. Mathematical modelling of a primary zinc/air battery, Journal of the Electrochemical Society, 139, 1105-1113.

Gilliam R., Graydon J., Kirk D., Thorpe S., 2007, A review of specific conductivities of potassium hydroxidesolutions for various concentrations and temperatures, International Journal of Hydrogen Energy, 32, 359–364.

Pei P., Wang K., Ma Z., 2014, Technologies for extending zinc-air battery's cycle life: A review, Applied Energy, 128, 315-324.

Sapkota P., Kim H., 2010, An experimental study on the performance of a zinc air fuel cell with inexpensive metal oxide catalysts and porous organic polymer separators, Journal of Industrial and Engineering Chemistry 16, 39–44.

Schröder D., Krewer U., 2014, Model based quantification of air-composition impact on secondary zinc air batteries, Electrochimica Acta, 117, 541–553.

Suren S., Kheawhom S., 2016, Development of a high energy density flexible zinc-air battery, Journal of the Electrochemical Society, 163, A846–A850.

Wongrujipairoj K., Poolnapol L., Arpornwichanop A., Suren S., Kheawhom, S., 2017, Suppression of zinc anode corrosion for printed flexible zinc-air battery, Physica Status Solidi (b), 254, 1600442.

Xiao Y., Jing R., Song H., Zhu N., Yang H., 2016a, Design and experiment on zinc-air battery continuous power controller based on microcontroller, Chemical Engineering Transactions, 51, 91-96.

Xiao Y., Zhang Q., Zhu N., Zhao H., Chen Z., 2016b, Control system of zinc-air battery continuous power generation device based on microcontroller, Chemical Engineering Transactions, 51, 61-66.

Xu M., Ivey D. G., Xie Z., Qu W., 2015, Rechargeable Zn-air batteries: Progress in electrolyte development and cell configuration advancement, Journal of Power Sources, 283, 358–371.